Eng. Sci., 2022, **19**, 167–174

Engineered Science

DOI: https://dx.doi.org/10.30919/es8d611

Disparity Map from Stereo Images for Three-dimensional Surface Reconstruction

Z. A. M. Nazmi,[1,#] Rostam Affendi Hamzah,[1,#,*] M. N. Zarina[2] and Z. Madiha[1]

Abstract

This article proposes a new disparity map algorithm for three-dimensional (3D) surface reconstruction. Fundamentally, this map provides important information, which is commonly used in autonomous vehicle navigation, 3D surface reconstruction, and virtual reality. The development of this map requires several important stages which start with matching cost computation, cost aggregation, optimization, and refinement stage. To develop an accurate disparity map, the framework must be robust against the challenging regions which are low texture, plain color, and repetitive pattern. Hence, the novelty of this work is to develop a new framework for the stereo-matching algorithm to improve the accuracy of these regions. This framework starts with the sum of squared difference (SSD) and the combination of two edge-preserving filters to increase the robustness against the challenging regions. The SSD convolves using the block matching technique to increase the efficiency of the matching process on the low texture and plain color regions. Moreover, two edge-preserving filters will increase the accuracy of the repetitive pattern region. The results show the framework is accurate and capable to work with these challenging regions. Moreover, this work is competitive with other published methods such as Adaptive Deconvolution Stereo Matching and Binary Stereo Matching.

Keywords: Disparity map reconstruction; Edge filter; Image processing; Stereo matching algorithm; Sum of squared differences.
Received: 23 September 2021; Revised: 04 January 2022; Accepted: 06 January 2022.
Article type: Research article.

1. Introduction

The disparity map contains important information for many applications such as range estimation, size measurement, and three-dimensional (3D) surface reconstruction. This article introduces disparity map estimation from stereo images which is part of the stereo vision field of study. Stereo vision is the most important field in computer vision, and it provides various algorithms for computing different image processing-related fields of study. Basically, these stereo images go through a stereo-matching process to get the disparity map. Based on several literature works[1] with previously published articles, the disparity map is also called a disparity map. The process is using two stereo images, the scene depth can be obtained from two separate points with some baseline displaced values. The correlation values of the left image compared with the right image are the result of stereo matching. The disparity map is determined using the different intensity of pixel values on the map or the output from the stereo matching process based on the disparity map.[2,3] The stereo-matching function for computing the exact disparity map is very challenging and difficult. The challenges are due to the repetitive pattern, low texture area, and plain color regions.[4] These regions are difficult to be matched with and remain a challenge for the researchers to get an accurate result.

The process of stereo-matching is one of the most interesting tasks in the computer vision research area. This process begins with the matching of corresponding points from two images (*i.e.*, left and right input images). Essentially, the framework of the matching process was proposed by Scharstein and Szeliski,[5] there are three major methods to develop the stereo-matching framework. The first is the local method which uses all four stages in developing the framework. The optimization of the local method employs a Winner-Takes-All (WTA) strategy. In difference, the global method uses an energy minimization approach from the Markov random field (MRF) technique. This method utilizes three stages which exclude the aggregation stage. The third method is semi-global, which this method combines both local and global methods. Semi-global employs all four stages.[6]

[1] *Fakulti Teknologi Kejuruteraan Elektrik & Elektronik, Universiti Teknikal Malaysia Melaka, Malaysia.*
[2] *Fakulti Kejuruteraan Elektronik & Kejuruteraan Komputer, Universiti Teknikal Malaysia Melaka, Malaysia.*
[#] *These authors contributed to this work equally.*
**E-mail:* rostamaffendi@utem.edu.my (R A Hamzah)

Commonly, the depth map of the global method is calculated by manipulating the global energy feature. Graph cuts (GC),[7] belief propagation (BP)[8], and dynamic programming (DP)[9] are the algorithms with the global method. Hosni *et al*.[9] developed an algorithm to identify the depth discontinuities from pairs of stereo images. Their approach was able to execute the dynamic programming acceleration.[10] A new stereo matching based on segmentation using graph cuts, which is used by assigning disparity planes to each segment to achieve the optimal solution.[11] These planes integrate the cost allocation of global energy minimization to support two stages of MRF modeling. This method has successfully solved the problem of stereo-matching in occlusion areas. While previous approaches can effectively yield precise disparities in stereo matching, it isn't easy to enforce them, and complex scenes may fail to implement them. In addition, the learning-based methods are not reliable but are dependent on the training data. Although high accuracy can be achieved for disparity estimation through global optimization, huge computation complexity and execution time also limit its implementation in real-time applications. Furthermore, the semi-global method is also implemented using the MRF approach where the framework is similar to the global method with the cost aggregation stage added to the framework.

Matching cost computation is the first stage that produces a preliminary disparity map. This stage generates high noise due to the corresponding process of left and right images at each coordinate. There are several available methods in current research such as pixel-based matching cost,[12] feature-based matching cost,[13] and block matching cost.[14] All of these techniques have their own advantages and disadvantages as stated.[15] Pixel-based is fast but produced high noise compared to the other matching cost techniques. The feature-based technique creates a sparse disparity map that only discovers image features such as edges or boundaries. The last matching cost technique is the block-based method which this method is able to produce high accuracy if the size of the windows is suitably selected. The aggregation stage for the stereo matching algorithm is very important to remove the preliminary noise after the matching cost process. In common, this stage is applied in local and semi-global methods. The aggregation process implements the filtering by summing or averaging the cost volume in a support window. Some of the available algorithms utilize segmentation to improve accuracy. The adaptive support windows are applied to increase the accuracy by adjusting the intensity of the neighboring pixel.[15] Žbontar and Le Cun[16] proposed non-local stereo matching using segment-tree to improve the disparity map accuracy and to reduce the execution time. In placing more emphasis, on works,[17-19] a cross-scale design was suggested to enhance the cost averaging for effective stereo matching. Recursive edge-aware (REAF)[20] filters are provided for precise and effective stereo matching.

The third stage is disparity optimization which this stage normalizes the disparity value and converts it to the intensity of the depth pixel on the map. Local-based methods embrace this stage with the same approach as implemented.[21] Global and semi-global methods as implemented[22] skip this stage due to these methods minimize the disparity with the energy minimization approach similar to the MRF technique. For the final stage of the stereo matching framework, the disparity map refinement stage is taking place. This stage removes the remaining noise on the disparity map as implemented.[23] It has two sequential processes at this stage which are invalid pixels detection and final disparity map improvement or filtering. The segment-based approach was utilized based on plane fitting from the initial depth pixel on each segment.[24] The assumption of depth pixels is varied smoothly and continuously within each homogeneous color segmentation to improve the accuracy. The rest of this paper is organized as follows. The next section explains the methodology of the proposed work in this article and is followed by the results and discussion. The last part is the conclusion of the performance work in this article.

2. Experimental section

The proposed framework in this article is displayed in Fig. 1. Stage 1: The matching process starts with the SSD cost function to get the preliminary disparity map. This function uses the size of a 19 × 19 window with a block-matching technique. Proper selection of window sizes produces more accurate results, and it should improve the efficiency of the corresponding process. Stage 2: At this stage, the preliminary disparity map will be filtered to remove the noise or invalid pixels. The guided filter (GF)[25] will be used in the framework. The GF is a type of edge-preserving filter that enhances the disparity map result. Hence, the use of this type of filter eliminates the invalid pixels on the disparity map and is capable to increase the accuracy. Stage 3: This stage introduces the optimization level of disparity selection. The proposed work in this article uses the WTA strategy where the normalization of disparity value is selected based on the minimum number. The final stage in the proposed framework is to further improve the accuracy through two continuous processes.

The processes fill in invalid pixels then followed by the final filtering process which uses the bilateral filter (BF).[26] The purpose of the fill-in process is to replace the invalid pixel with a neighboring valid pixel. This process makes the disparity map more accurate and is capable to reduce the error on the disparity map. The BF is used in the framework since this filter is able to remove the remaining noise and preserved the object edges. The capability of this filter at this stage is to upsurge the accuracy of the final disparity map.

2.1 Matching cost computation

The SSD is used in the proposed framework as shown in Fig. 1 which this stage produces a preliminary disparity map. Thus, the early stage is very important where the corresponding

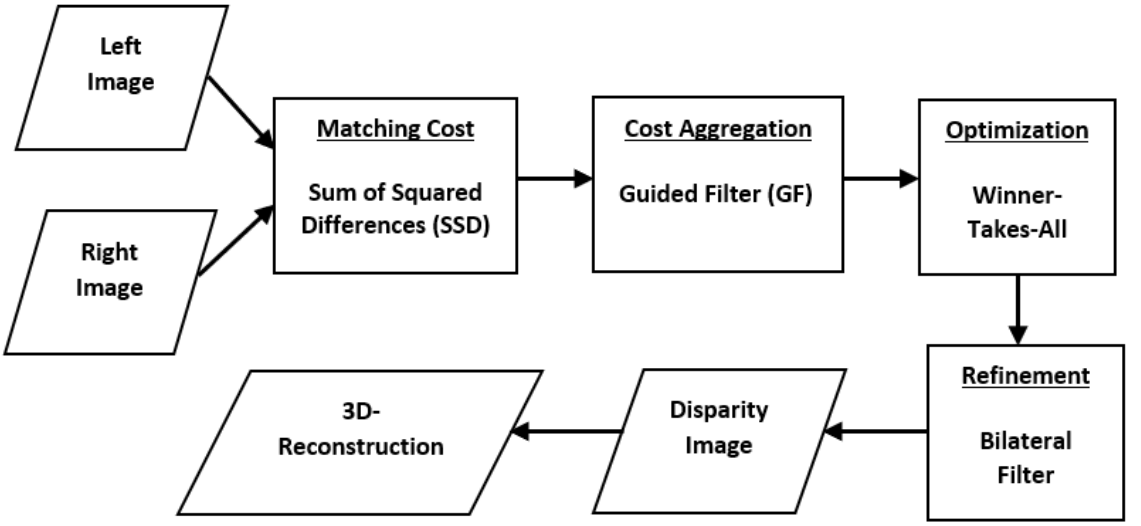

Fig. 1 A diagram of the proposed algorithm.

points between two pixels of left and right images take place. One of the major problems for the matching process at this the stage is corresponding points on the low texture regions. To minimize the mismatched problem during the matching process, the block matching technique or window-based technique is applied in this framework with the SSD function. The advantage of the block matching technique is capable to reduce the noise in the low texture region. The consistency of weight at every pixel in the SSD windows increases the matching correctness and at the same time reduces the mismatched error. Equation (1) shows the SSD function in which the RGB images are used as input stereo images.

$$SSD(x,y,d) = \frac{1}{M}\sum_{(x,y)\in M}|I_l^i(x,y) - I_r^i(x-d,y)|^2 \quad (1)$$

where the (x,y,d) is the pixel of interest with the disparity value, the left, and right images are I_l, and I_r respectively, the RGB channels are denoted by i of right and left images, and the SAD support window size represented by M at the size of (19 × 19).

2.2 Cost aggregation

This stage is the most important part which removes the noise from the preliminary depth map. Fundamentally, this stage will filter out the noise from the matching process and should be proficient to keep the object edges. Some illogical and ambiguous pixels are formed during the corresponding process. Therefore, at this step, the filter must be strong and robust against any error at this stage. The GF is employed due to deeply maintain object boundaries and at a similar time capably eliminate noise, particularly on the low texture and flat color regions. Equation (2) is the equation of GF applied in this paper.

$$GF_{(p,q)}(I) = \frac{1}{w^2}\sum_{(p,q)\in w_c}\left(1 + \frac{(I_p-\mu_c)(I_q-\mu_c)}{\sigma_c^2+\varepsilon}\right) \quad (2)$$

where $\{\varepsilon, \sigma, \mu, I, p, q, w, c\}$ denoted by {center pixel of w, variance value, constant parameter, reference image (left input image), mean value, coordinates of (x, y), window support size, neighboring coordinates}. The GF is engaged in this paper in line for efficient noise removal with fast execution of time processing. The GF improves the precision at the object boundaries. The final calculation of this step is provided by Equation (3):

$$CA(x,y,d) = SSD(x,y,d)GF_{(p,q)}(I) \quad (3)$$

where the CA is the cost aggregation, SSD (x,y,d) signifies the input of the first stage, and $GF_{p,q}(I)$ signifies the kernel of the GF.

2.3 Disparity optimization

This stage optimizes the disparity map by using the WTA strategy. The strategy involves the selection of the minimum disparity value that is normalized by using the floating-point number from the cost aggregation stage. The WTA is normally used in local-based methods due to fast implementation.[18,26] The WTA calculation is given by Equation (4).

$$d_{x,y} = arg\ CA(x,y,d) \quad (4)$$

where C(x,y,d) denotes the second stage of the aggregation step and D represents a set of valid disparity values for an image. Basically, after this stage, the disparity map still includes noise or invalid pixels. Thus, this map needs to be enhanced or to be refined to get the best results.

2.4 Refinement stage

This stage is the last part of the proposed algorithm which has two continuous post-processes. It starts with the hole filling process or technically the process of invalid pixel replacement with the valid pixel value. This article uses the nearest valid pixel value (*i.e.*, close neighbor) to fill in the hole or to replace the invalid pixel locations. After this process, some unwanted pixels or artifacts emerged. Therefore, the disparity map needs to be smoothed to filter out the artifacts. Thus, the Bilateral Filter (BF) is utilized. This filter is very robust against the low texture and repetitive pattern regions. It is because the characteristic of this filter is able to remove the noise and at the same time preserved the object edges. The BF function is shown by Equation (5) as follows:

$$BF_{p,q} = \sum_{q \in w_B} exp\left(-\frac{|p-q|^2}{\sigma_s^2}\right) exp\left(-\frac{|I_p - I_q|^2}{\sigma_c^2}\right) \quad (5)$$

where w_B is the windows that support the size of BF and q represents the neighboring pixels and p is the location pixel of interest at (x,y) respectively. The p-q represents spatial Euclidean interval and I_p-I_q signifies the Euclidean distance in color space. The σ_s indicates a factor of spatial adjustment and σ_c corresponds to the similarity factor for color detection. Therefore, the final result of the disparity map is represented by Equation (5) which the $BF_{p,q}$ is the depth output d at the location pixel of interest p.

2.5 3D Surface reconstruction

This section explains the application of the disparity map. It will prove the accuracy of the proposed disparity map in this article based on qualitative measurement. From the depth, map result in Equation (5), a library from the OpenCV will be utilized for 3D surface reconstruction. It is based on Equation (6):

$$D = \frac{bf}{d} \quad (6)$$

where D represents the depth, b and f are the stereo camera baseline and focal values respectively, and d denotes the disparity value. Therefore, the 3D surface reconstruction in this article is formulated as Equation (7) as follows:

$$3D = \frac{bf}{BF_{p,q}} \quad (7)$$

3. Results and discussion

This section describes the experimental results and discussion the performance of the proposed framework. The experiment has been conducted based on the C++, 10 Gen Intel Core i5 processor, and 8 GHz Read Access Memory (RAM). The standard benchmarking dataset used in this article is provided by the Middlebury Stereo Evaluation system. This database contains 30 images of training and testing images which these images have different characteristics such as various illumination, low texture, discontinuity, and plain color regions. All and nonocc errors are the attributes of the performance measurement of the proposed algorithm. The measurement is based on the weight average error of testing and training images which is provided by the Middlebury online webpage. Fig. 2 illustrates the disparity map results in the grayscale color of the challenging regions. The results from Fig. 2 show 3 images with clear matching results on the disparity map. The low texture region of the chair on the Adirondack image is clearly observed in the disparity map result.

The plain color region of recycle bin image is also visible on the disparity map. For the repetitive region, the Jade plant

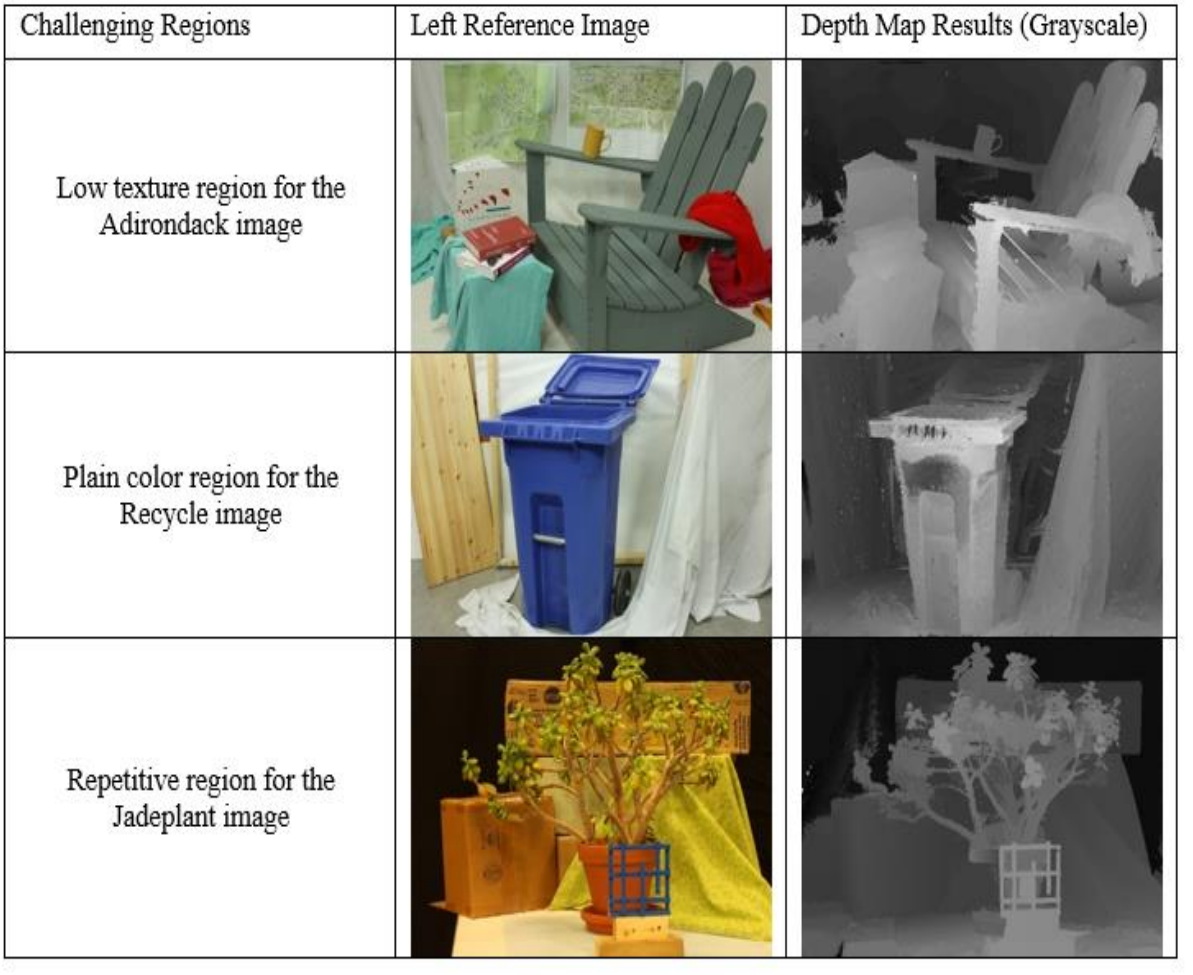

Fig. 2 The disparity map results for the challenging regions using training images.

image is selected due to its repetitive leaves on the image. The disparity map result shows the leaves are well detected with their object sizes. Based on this figure, the proposed work in this article is strong against the challenging regions. Overall, 15 training images have been used for performance measurement. There are Recycle, Adirondack, Teddy, Playroom, Jade plant, MotorcycleE, Pipes, Piano, PianoL, Playtable, ArtL, PlaytableP, Shelves, Motorcycle, and Vintage as displayed in Fig. 3. This figure shows almost accurate disparity map results that were constructed based on RGB color channels. Fundamentally, the red color indicates the object is closer to the stereo camera. Meanwhile, the blue color region is far away from the stereo camera. It is also applied to the disparity map with the grayscale color scheme.

Table 1 and Table 2 are the quantitative measurement results based on the proposed work in this article using the Middlebury standard stereo evaluation system. There are 15 training images with the quantitative results provided by Middlebury through the online system. Table 1 tabulates the results of the *nonocc* error which also displays that the proposed algorithm produces 8.89% of the average error. It ranks second behind the MPSV[18] method with 8.81% and is more accurate than the ADSM[19] and BSM[26] methods with 8.95% and 13.40% respectively. For Table 2, all error is presented where the evaluation is made with the same methods in Table 1 to make the comparison process more consistent. The proposed work produces the lowest average error compared to the ADSM,[19] BSM[26] and more importantly, the proposed work is more accurate than the MPSV.[18] It shows that the proposed work in this article is competitive with other available methods. There are several complex images such as Jadeplant, Piano, PianoL, and Playtable that produce the lowest average error compared with other methods in Table 2.

Figure 4 demonstrates the results of 3D surface reconstruction from a disparity map result. Fundamentally, the accuracy of the disparity map produced by the proposed framework is very crucial. It determines the quality of 3D surface reconstruction and overall algorithm features. Based on this figure, the recycle disparity map (grayscale) is obviously discovered where the contour of depth detection is accurately presented for both conditions (*i.e.*, front view and top view). The recycle box is closer to the stereo camera and is clearly separated from the background grayscale tones. It shows that the background objects are far away from the recycle box position. It can be proved by the 3D surface reconstruction from the side view image where the depth distance is well-positioned. The depth layers are also shown in this image which indicates the matching process from the first

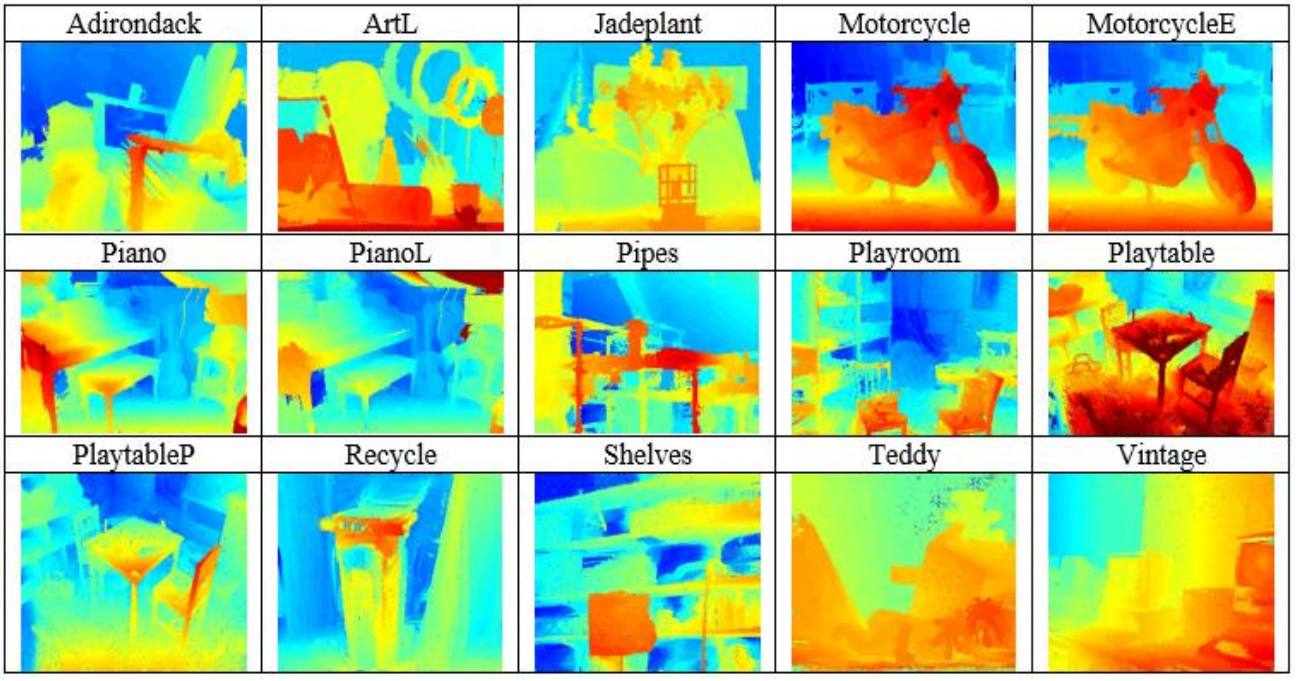

Fig. 3 The disparity map results from the proposed work using the training images.

Table 1. The comparison of currently available methods with the nonocc error from the Middlebury.

Algorithms	Avg	Adiron	ArtL	Jadepl	Motor	MotorE	Piano	PianoL	Pipes	Playrm	Playt	PlayP	Recyc	Shelvs	Teddy	Vintge
MPSV[18]	8.81	3.83	6.00	19.70	5.85	5.53	5.68	34.30	9.59	5.86	15.30	4.20	4.59	13.00	3.70	14.30
Proposed Algorithm	8.89	7.17	7.14	15.1	4.76	5.57	6.98	12.75	9.66	14.82	9.89	7.74	7.92	18.19	5.17	17.25
ADSM[19]	8.95	13.30	6.10	15.00	3.67	5.67	7.08	20.60	6.57	13.20	23.10	3.55	5.76	17.20	3.05	10.10
BSM[26]	13.40	7.27	11.40	30.50	6.67	6.52	10.80	32.10	10.50	12.50	24.40	12.80	7.42	16.40	4.88	32.80

Table 2. The comparison of current available methods with the *all* error from the Middlebury.

Algorithms	Avg	Adiron	ArtL	Jadepl	Motor	MotorE	Piano	PianoL	Pipes	Playrm	Playt	PlayP	Recyc	Shelvs	Teddy	Vintge
Proposed Algorithm	12.21	9.54	10.87	30.97	7.41	8.25	7.00	14.54	15.59	19.34	11.98	9.86	8.91	17.11	5.91	17.65
ADSM[19]	12.30	14.30	10.60	34.10	6.00	8.00	7.37	20.40	12.10	16.90	25.50	5.84	5.83	17.20	4.11	11.10
MPSV[18]	12.70	5.87	9.43	40.20	9.11	8.80	7.03	34.20	15.80	8.58	16.90	5.89	6.78	13.70	4.82	16.80
BSM[26]	23.50	12.70	28.70	58.70	14.80	14.70	16.00	35.80	24.50	29.40	31.00	20.20	12.10	19.20	14.30	39.30

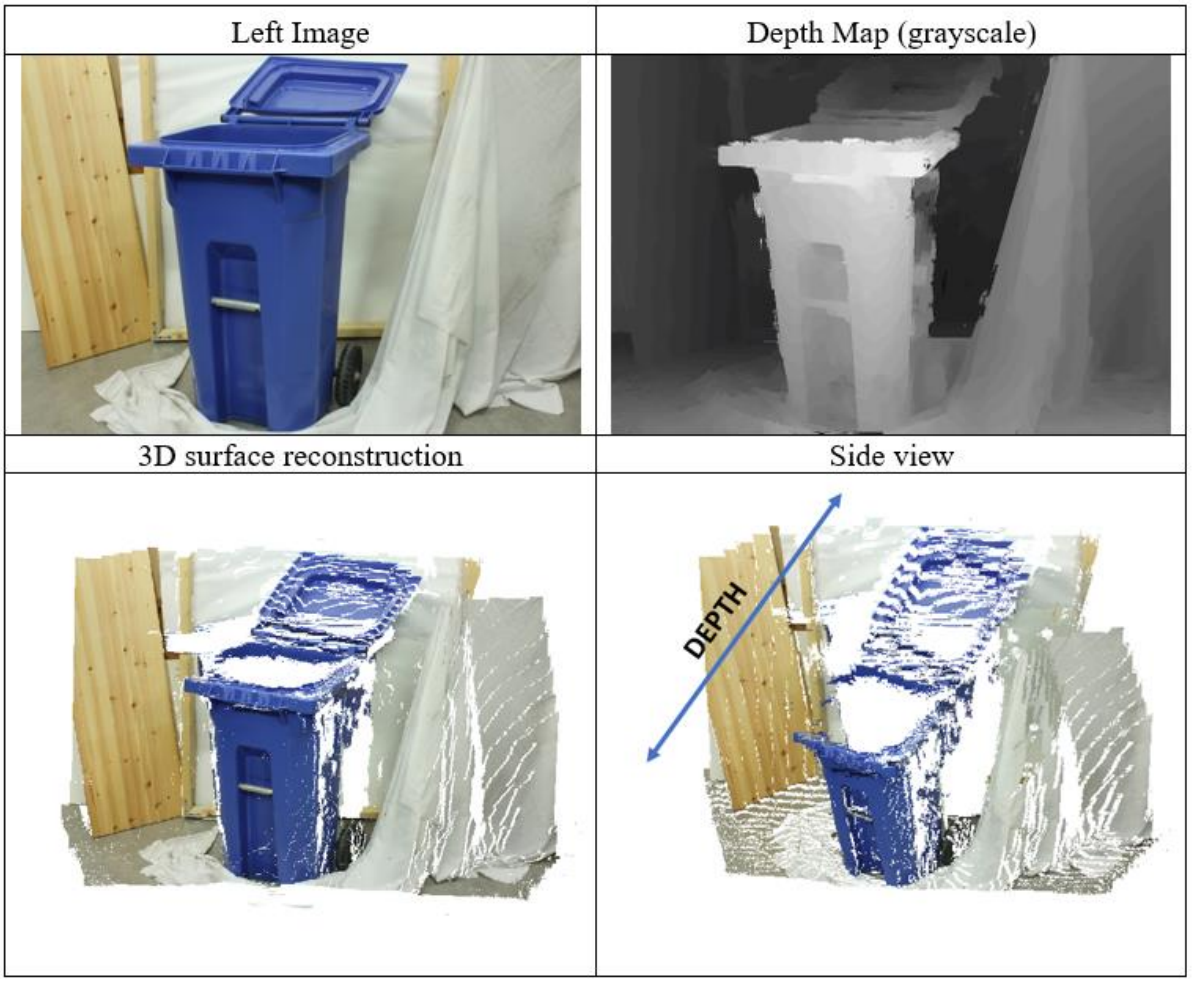

Fig. 4 The disparity map results from the proposed work using the training images.

to the final stage of the proposed work is efficiently established. Fundamentally, the pixel intensities are accurately positioned on the disparity map of each object. Hence, this helps to accurately reconstruct the 3D surface with accurate depth estimation.

4. Conclusions

This article proposes an algorithm for disparity map reconstruction using stereo images. This work established four stages of algorithm framework producing disparity map or disparity map. The framework starts with matching cost computation, cost aggregation, optimization, and refinement stage. The proposed work in this article used SSD, GF, WTA, and BF respectively. Based on the experimental analysis, the proposed work in this article is capable to work with the regions that have difficulty being matched such as low texture, plain color, and repetitive pattern regions. It can be proved in Fig. 1 above; the disparity maps are completely reconstructed using sample standard images. The performance of the proposed framework is also measured based on the quantitative measurement which is provided in Table 1 and Table 2. From these tables, it can be seen the proposed work is competitive with current published works with 8.83% and 12.21% of nonocc and all errors respectively. These quantitative measurements are provided by the standard benchmarking system from Middlebury. Finally, this proposed work is also capable to be used for 3D surface reconstruction which is presented in Fig. 4 using Recycle image. The depth

estimation from the 3D reconstruction results shows the precise object's location and depth contour. Hence, the proposed work in this article can be used as a complete algorithm for the disparity map algorithm and is viable with other available methods.

Acknowledgments
This work was sponsored by the Universiti Teknikal Malaysia Melaka and the Ministry of Higher Education Malaysia with grant number FRGS/1/2020/TK0/UTEM/02/12.

Conflict of interest
There are no conflicts to declare.

Supporting information
Not Applicable.

References
[1] R. A. Hamzah, A. F. Kadmin, S. F. A. Gani, K. A. Aziz, T. M. F. T. Wook, N. Mohamood, M. G. Y. Wei, *Bulletin of Electrical Engineering and Informatics*, 2021, **10**, 111-117, doi: 10.11591/eei.v10i1.1947.
[2] W. Budiharto, A. Santoso, D. Purwanto, A. Jazidie, *TELKOMNIKA (Telecommunication Computing Electronics and Control)*, 2011, **9**, 433, doi: 10.12928/telkomnika.v9i3.733.
[3] E. Winarno, A. Harjoko, A. M. Arymurthy, E. Winarko, *International Journal of Electrical and Computer Engineering (IJECE)*, 2016, **6**, 2818, doi: 10.11591/ijece.v6i6.12970.
[4] R. A. Hamzah, H. Ibrahim, A. H. A. Hassan, Stereo Matching Algorithm for 3D Surface Reconstruction Based on Triangulation Principle, *2016 1st International Conference on Information Technology, Information Systems and Electrical Engineering (ICITISEE)*, 2016, 119-124, doi: 10.1109/ICITISEE.2016.7803059.
[5] D. Scharstein, R. Szeliski, A taxonomy and evaluation of dense two-frame stereo correspondence algorithms. *International Journal of Computer Vision*, 2002, **47**, 7-42, doi: 10.1023/A:1014573219977.
[6] H. Xi, W. Cui, Wide baseline matching using support vector regression, *Telkomnika*, 2013, **11**, 597-602. doi: 10.12928/TELKOMNIKA.v11i3.1042.
[7] I. Vedamurthy, D. C. Knill, S. J. Huang, A. Yung, J. Ding, O. S. Kwon, *Philosophical Transactions of the Royal Society B: Biological Sciences*, 2016, **371**, 1-13, doi: 10.1098/rstb.2015.0264.
[8] D. Damen, D. C. Hogg, Recognising linked events: searching the space of feasible explanations, *Computer vision and pattern recognition (CVPR)*, 2009, doi: 10.1109/CVPR.2009.5206636.
[9] A. Hosni, C. Rhemann, M. Bleyer, C. Rother, M. Gelautz, Fast cost-volume filtering for visual correspondence and beyond, *IEEE Transactions on Pattern Analysis and Machine Intelligence*, 2013, **35**, 504-511, doi: 10.1109/tpami.2012.156.
[10] C. Wu, J. Song, G. Ma, Y. Zhang, J. Sun, F. Zhang, *Remote Sensing Letters*, 2021, **12**, 869-878, doi: 10.1080/2150704x.2021.1944690.
[11] R. A. Hamzah, H. Ibrahim, *Electronics Letters*, 2018, **54**, 876-878, doi: 10.1049/el.2017.3956.
[12] C. Richardt, H. Kim, L. Valgaerts, C. Theobalt, Dense Wide-Baseline Scene Flow from Two Handheld Video Cameras, *Fourth International Conference on 3D Vision (3DV)*, 2016, 276-285, doi: 10.1109/3DV.2016.36.
[13] Q. Liang, Y. Yang, B. Liu, Stereo matching algorithm based on ground control points using graph cut, *7th International Congress on Image and Signal Processing*, IEEE, 2014, 503-508, doi: 10.1109/CISP.2014.7003832.
[14] Q. Yang, P. Ji, D. Li, S. Yao, M. Zhang, *Image and Vision Computing*, 2014, **32**, 202-211, doi: 10.1016/j.imavis.2014.01.001.
[15] J. Kowalczuk, E. T. Psota, L. C. Perez, Real-time stereo matching on CUDA using an iterative refinement method for adaptive support-weight correspondences, *IEEE Transactions on Circuits and Systems for Video Technology*, 2013, **23**, 94-104, doi: 10.1109/tcsvt.2012.2203200.
[16] J. Žbontar, Y. LeCun, Computing the stereo matching cost with a convolutional neural network, *IEEE Conference on Computer Vision and Pattern Recognition*, 2015, 1592-1599. doi: 10.1109/CVPR.2015.7298767.
[17] H. Hirschmüller, P. R. Innocent, J. Garibaldi, *International Journal of Computer Vision*, 2002, **47**, 229-246, doi: 10.1023/a:1014554110407.
[18] N. Ma, Y. Men, C. Men, X. Li, *Symmetry*, 2016, **8**, 159, doi: 10.3390/sym8120159.
[19] M. Kitagawa, I. Shimizu, R. Sara, High accuracy local stereo matching using DoG scale map, *Fifteenth IAPR International Conference on Machine Vision Applications*, 2017, 258-261. doi: 10.23919/MVA.2017.7986850.
[20] R. A. Hamzah, M. G. Y. Wei, N. S. N. Anwar, Stereo matching based on absolute differences for multiple objects detection, *TELKOMNIKA (Telecommunication Computing Electronics and Control)*, 2019, **17**, 261-267, doi: 10.12928/TELKOMNIKA.v17i1.9185.
[21] S. S. Wu, C. H. Tsai, L. G. Chen, Efficient Hardware Architecture for Large Disparity Range Stereo Matching Based on Belief Propagation, *IEEE International Workshop on Signal Processing Systems*, 2016, 236–241, doi: 10.1109/SiPS.2016.49.
[22] A. F. Kadmin, R. A. Hamzah, N. A. Manap, M. S. Hamid, *Advances in Mathematics: Scientific Journal*, 2020, **10**, 743-758, doi: 10.37418/amsj.10.2.6.
[23] H. Hirschmüller. D. Scharstein, Evaluation of Cost Functions for Stereo Matching, *IEEE Conference on Computer Vision and Pattern Recognition*, IEEE, 2007, doi: 10.1109/CVPR.2007.383248.
[24] N. Einecke, J. Eggert, Anisotropic Median Filtering for Stereo Disparity Map Refinement, *International Conference on Computer Vision Theory and Applications*, 2013, 189-198, doi: 10.5220/0004200401890198.
[25] A. Geiger, M. Roser, R. Urtasun, Efficient Large-Scale Stereo Matching, *Asian Conference on Computer Vision*, 2011, 25-38. doi: 10.1007/978-3-642-19315-6_3.
[26] N. Zheng, G. Loizou, X. Jiang, X. Lan, X. Li, Computer

vision and pattern recognition, *International Journal of Computer Mathematics*, 2007, **84**, 1265-1266, doi: 10.1080/00207160701303912.

Author Information

Z. A. M. Nazmi *currently pursuing the M.Sc. degree in Electronic Engineering from Universiti Teknikal Malaysia Melaka. His current research interests focusing on stereo vision and digital image processing. He is also interested in electronic soldering and circuit.*

Rostam Affendi Hamzah *graduated from Universiti Teknologi Malaysia where he received his B.Eng majoring in Electronic Engineering. Then he received his M. Sc. majoring in Electronic System Design Engineering and PhD majoring in Electronic Imaging from the Universiti Sains Malaysia. Currently he is a lecturer in the Universiti Teknikal Malaysia Melaka teaching digital electronics, digital image processing and embedded system.*

M. N. Zarina *received the Ph.D. degree from Universiti Putra Malaysia. She is currently a senior lecturer at Universiti Teknikal Malaysia Melaka. Her research interest includes image processing and computer embedded system engineering.*

Z. Madiha *was born in Melaka, Malaysia. She received the Bachelor degree in Electrical & Electronic Engineering from University Technology of Petronas in 2006 and Master of Engineering in Industrial Electronic and Control from University of Malaya.*

